

Influence of Cavitation in Seawater on the Etching Attack of Manganese-Aluminum-Bronzes

Paul Linhardt^{1,a}, Maria Victoria Biezma^{2,b}, Susanne Strobl^{1,c}
and Roland Haubner^{1,d*}

¹TU Wien, Institut für Chemische Technologien und Analytik,
Getreidemarkt 9/164-CT, A-1060 Vienna, Austria

²Universidad de Cantabria, Dpt. Ciencia e Ingeniería del Terreno y de los Materiales,
E.T.S. Náutica, Dique de Gamazo 1, Santander, Spain

^apaul.linhardt@tuwien.ac.at, ^bmaria.biezma@unican.es, ^csusanne.strobl@tuwien.ac.at,
^{d*}roland.haubner@tuwien.ac.at

Keywords: manganese-aluminum-bronze; cavitation; etching; seawater.

Abstract. During cavitation investigations with manganese-aluminum-bronzes (MAB) in seawater using ultrasound (US), it was found that the microstructure of the bronze was developed by etching. To investigate this phenomenon in more detail, metallographically polished MAB samples were US-treated in synthetic seawater. On the one hand, pulsed ultrasound was used with a sonotrode in order to be able to observe the effects of cavitation. On the other hand, an ultrasonic bath with less power than the sonotrode was used to investigate the influence of ultrasound on the electrochemical response of the MAB. It was found that the κ -phase is attacked most severely by cavitation, followed by β -phase and the α -phase. Potentiostatic measurements indicated that the transport of oxygen to, and of metal ions from the metal surface is enhanced by the ultrasound, which then leads to increased corrosion rates.

Introduction

Bronzes show excellent corrosion resistance, also in sea water, and are frequently used in many applications where corrosion, erosion and cavitation can occur. Typical examples are ship propellers, pumps, and turbines in hydropower plants. For such applications, the use of high-quality nickel-aluminum-bronze (NAB) or manganese-aluminum-bronze makes sense [1, 2]. Due to the complex alloy compositions, these bronzes have a multi-phase structure [3], which affects the corrosion behavior. There already exist numerous studies related to NAB [4 - 6], but less on MAB [7 - 9].

The microstructures of these bronzes mainly consist of three easily distinguishable phases (α , β and κ). The phases α and β form the matrix in which the κ -phase is embedded. Through heat treatments it is possible to influence the phase fractions, but also their size, geometry and distribution [2, 10 - 12].

For the use of bronzes in applications where cavitation occurs, it is important to understand the attack of the aqueous medium on the different phases of the microstructure [13]. During cavitation investigations with MAB in seawater, it was found that the microstructure of the bronze was developed by etching [14].

To investigate this phenomenon in more detail, metallographically polished MAB samples were treated in a beaker filled with synthetic seawater by pulsed ultrasound or by an ultrasonic bath.

Experimental Procedure

A MAB of the type CuMn12Al7Fe4Ni2 (analysis mass. %: 72 % Cu, 12 % Mn, 7 % Al, 4 % Fe, 2 % Ni, 2 % Zn, 0.08 Si, 0.02 Pb, 0.01 Sn) was subjected to examinations.

Metallography. The samples were embedded in epoxy resin. Metallographic preparation started with a plane-grinding disc (P220), followed by polishing with 9 – 1 μm diamond suspensions.

The etchants Klemm 1, $(\text{NH}_4)_2\text{CuCl}_4$, FeCl_3 , and $\text{NH}_3\text{-H}_2\text{O}_2$ were used to develop the microstructures [15].

The various samples were investigated by a light optical microscope (LOM), a scanning electron microscope (SEM) and by energy dispersive X-ray analysis (EDX).

Ultrasonic treatments. Synthetic seawater (SSW) with the ingredients – $\text{NaCl} + \text{MgCl}_2 \cdot 6\text{H}_2\text{O} + \text{CaCl}_2 \cdot 2\text{H}_2\text{O} + \text{MgSO}_4 \cdot 7\text{H}_2\text{O} + \text{NaHCO}_3$ (see DIN 50905-4, section 4.1.) – was used for the investigations.

Polished MAB samples were treated with the sonotrode (Fig. 1a) with different power and time and then the etching effects were photographed.

During the tests in the ultrasonic bath (Fig. 1b) electrochemical measurements could be carried out in parallel by using electrically contacted samples, a counter- and a reference-electrode, all connected to a potentiostat.

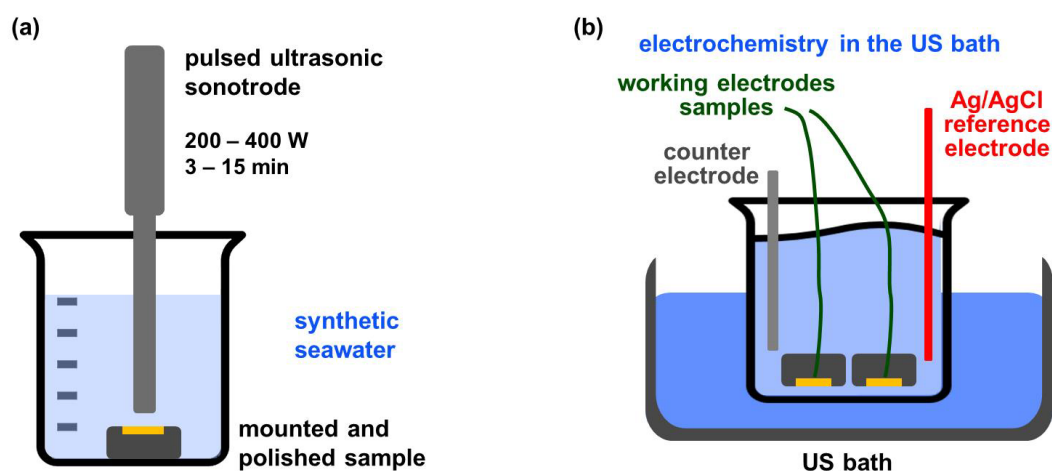


Fig. 1 Schemes of the experimental setups. (a) ultrasound applied by a sonotrode, (b) ultrasonic bath.

Results and Discussions

Conventional etching. For comparison purposes, MAB samples were treated with conventional etchants (Fig. 2).

With Klemm 1, the α -phase appears orange, the β -phase light brown and the κ -phases dark brown.

With $(\text{NH}_4)_2\text{CuCl}_4$, the α -phase is light brown, the β -phase is medium brown, and the κ -phases are white.

The FeCl_3 etching reveals the κ -phases as dark precipitations, whereby the remaining structure is attacked only very weakly.

$\text{NH}_3\text{-H}_2\text{O}_2$ etches the α -phase darker than the β -phase and the κ -phase is white.

Cavitation with Sonotrode. MAB shows localized attack, with the etching effects increasing with increasing duration of the ultrasonic treatment (Fig. 3).

It is striking that halos of corrosion products are formed around the iron- and manganese-rich κ -phases (Fig. 4a). In some cases, holes are found at typical locations of the κ -phase, which indicates that κ -phases may break out over the course of the ultrasonic treatment (Fig. 4b, c). It is assumed that the vapor bubbles required for cavitation are formed preferentially at the harder κ -phase, causing the destructive cavitation impacts there. In Fig. 4c a cracked top layer is visible.

SEM-EDX element mapping indicates an increased presence of O and Al around the regions with damaged κ -phase (Fig. 5), which is due to the locally increased corrosion attack and the deposition of corrosion products in the vicinity.

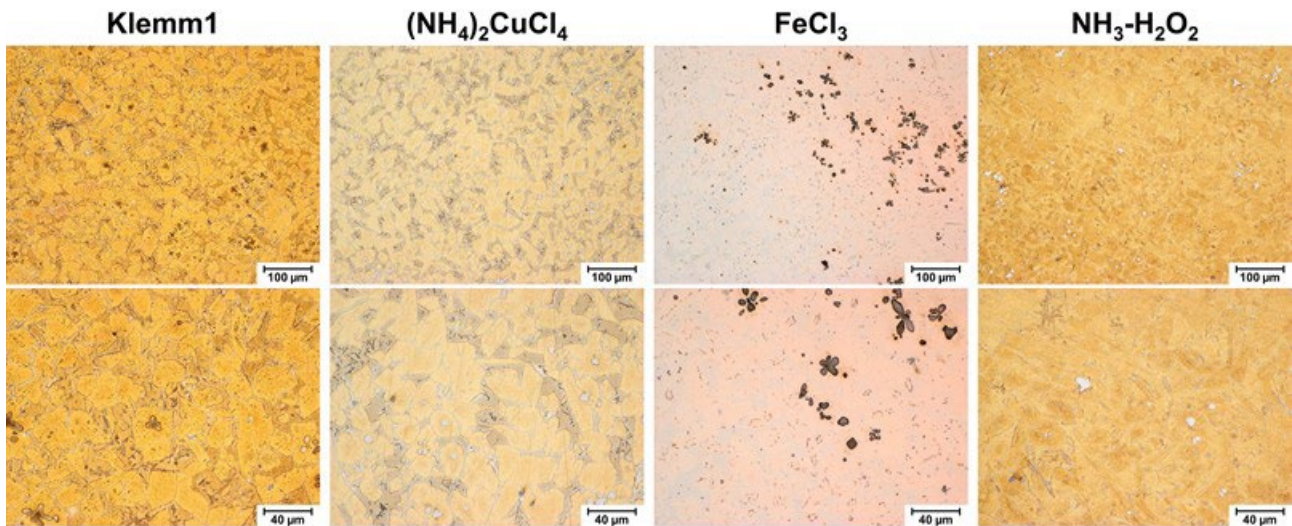


Fig. 2 Compilation of different etched structures received by applying conventional etchants.

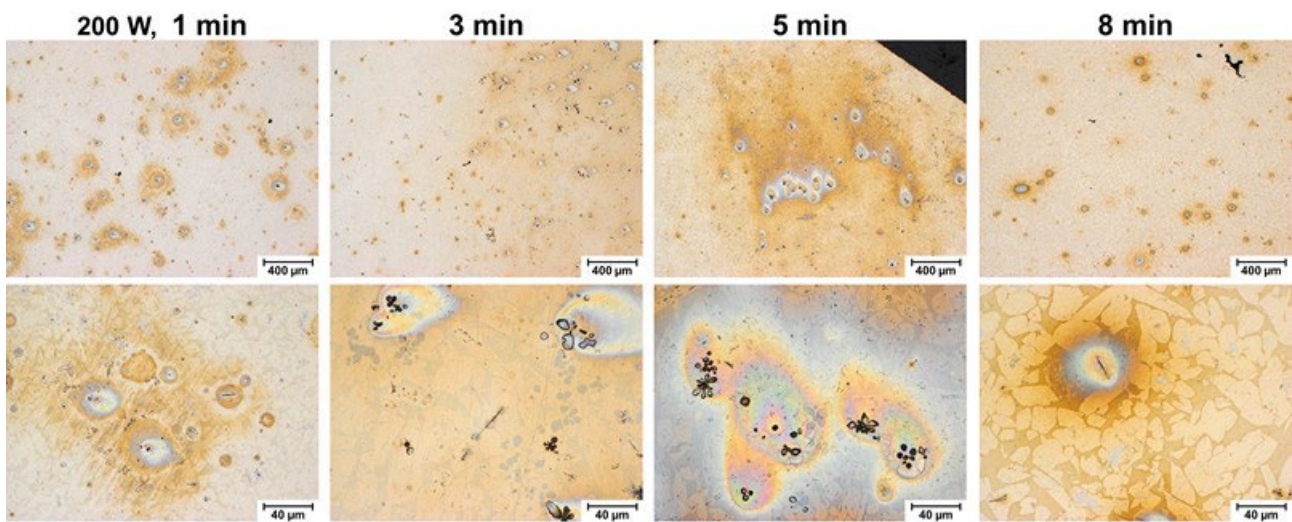


Fig. 3 MAB surfaces after ultrasonic treatment with the sonotrode in SSW. Ultrasonic power 200 W, variable duration.

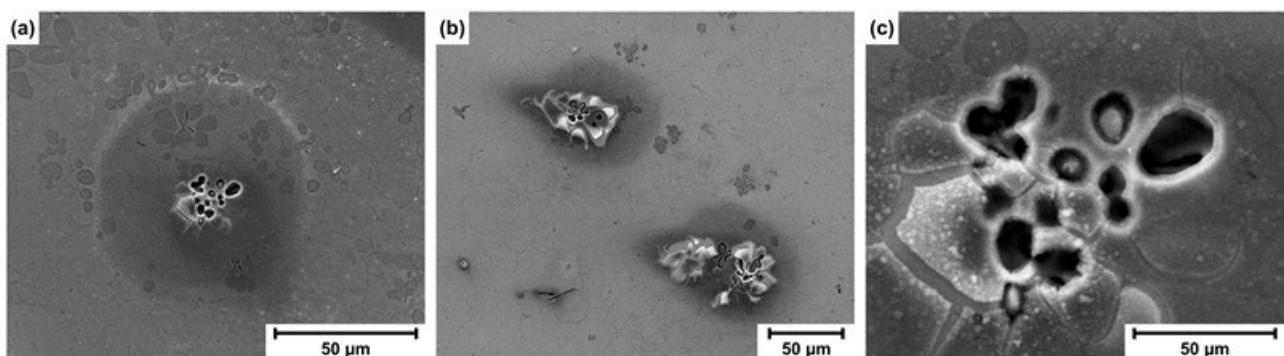


Fig. 4 MAB surface in SEM after ultrasound treatment with the sonotrode. (a, b) halos around clusters of κ -phase, (c) voids instead of κ -phase, and a cracked top layer is also evident.

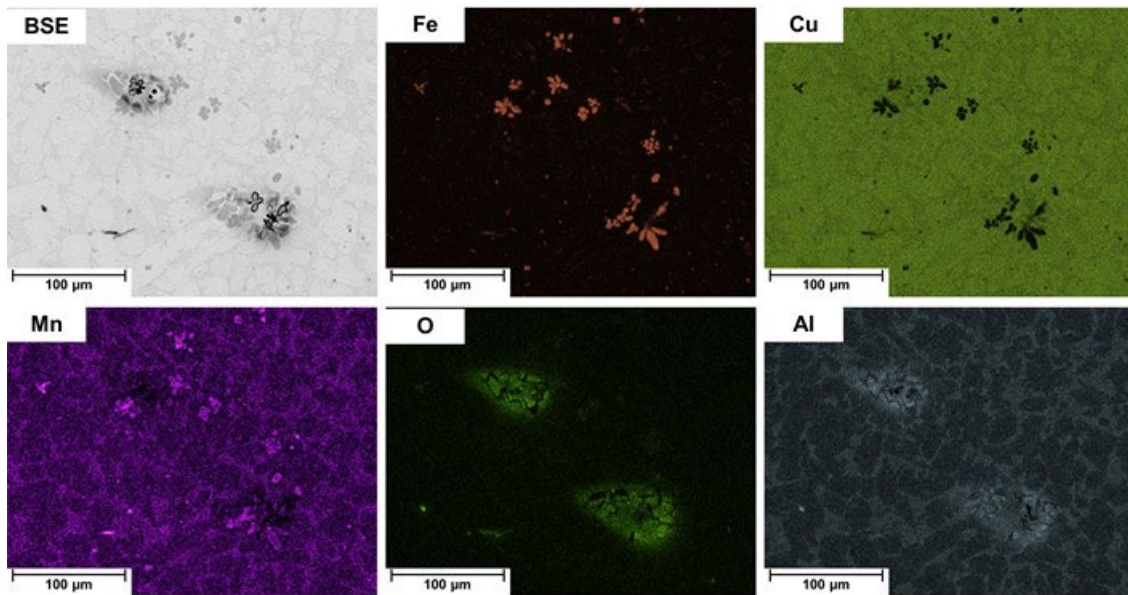


Fig. 5 SEM-EDX element mapping of MAB surface after sonotrode ultrasound treatment in SSW.

Cavitation with Ultrasonic Bath and Cathodic Polarization. The etching attack in the ultrasonic bath is more evenly distributed (Fig. 6) and slower compared to the tests with the sonotrode. The cathodic polarization used certainly also has a certain effect.

After this treatment, the κ -phase appears dark brown and the β -phase darker than the α -phase. In comparison with the conventional etchants, the etched pattern matches most closely that of the $(\text{NH}_4)_2\text{CuCl}_4$ etch, see Figure 2.

Weakly developed halos around κ -phase clusters can also be seen here, which indicates that vapor bubbles are also formed preferentially at the κ -phase in the less powerful ultrasonic bath.

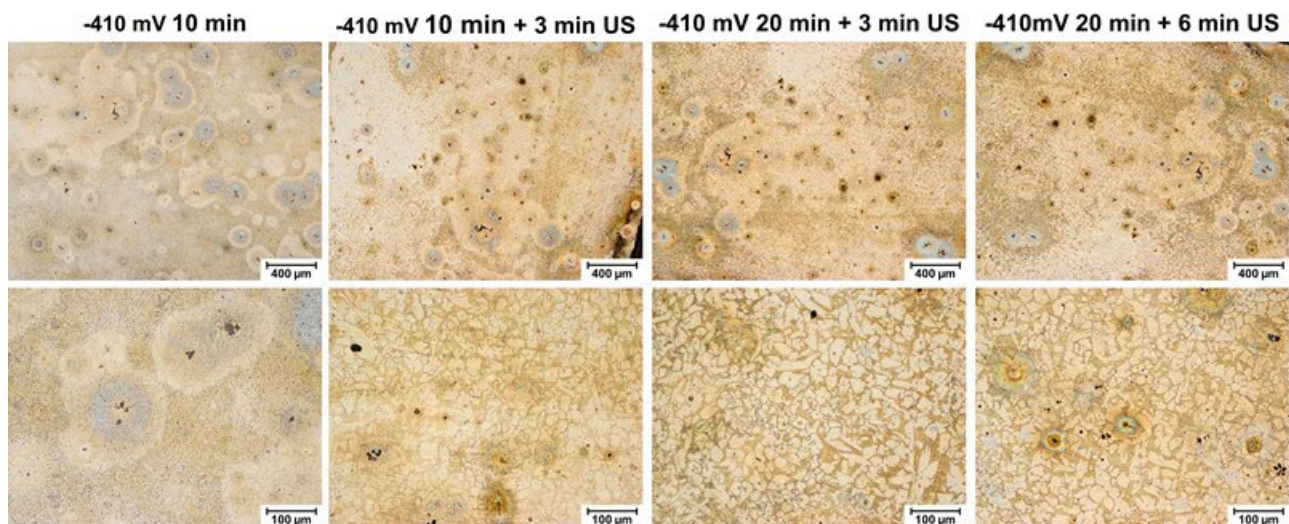


Fig. 6 MAB surfaces after various ultrasound treatments and cathodic polarization.

Electrochemistry with Ultrasonic Bath. The free corrosion potential (open-circuit potential E_{OC}) of MAB in SSW with and without US was found to increase during the ultrasonic treatment (Fig. 7). Applying mixed potential theory, this potential shift may be explained by US-enhanced oxygen supply to the corroding metal surface, while the metal dissolution is increased to lesser extent by the enhanced removal of metal ions from the surface.

At a potential below the free corrosion potential (cathodic polarization, -400 mV), an increase in the cathodic current is evident during US due to the enhanced oxygen supply (Fig. 8a). The presence of a protective layer from pre-corrosion has no influence here.

In the case of potentiostatic measurements under anodic polarization ($-250 \text{ mV}_{\text{Ag}/\text{AgCl}}$), MAB dissolves faster under US (Fig. 8b), resulting in increased anodic current due to enhanced removal of metal ions from the surface. This effect is much smaller for the sample which was pre-corroded for 18 h in SSW due to some protective layer which is not destroyed so quickly by cavitation impacts.

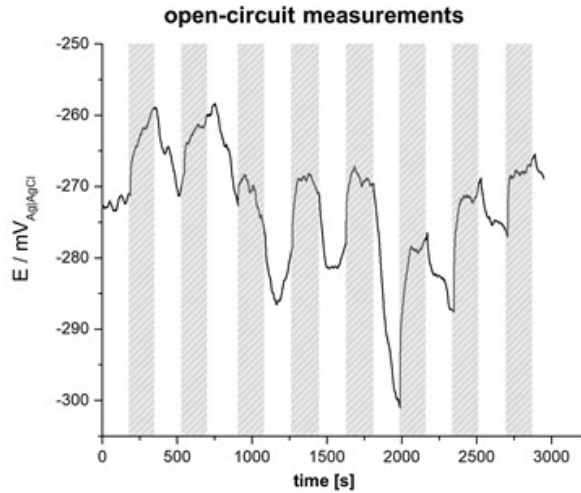


Fig. 7 Open-circuit potential E_{OC} [mV] of MAB in SSW with (hatched) and without (blank) US.

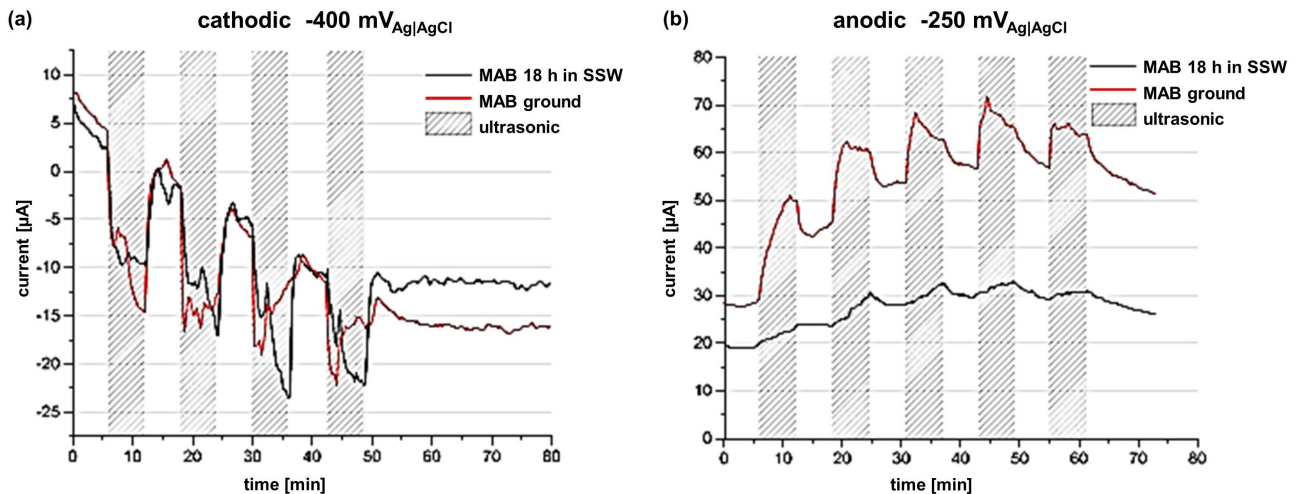


Fig. 8 Potentiostatic measurements of MAB in SSW with (hatched) and without (blank) US. (a) cathodic range $-400 \text{ mV}_{\text{Ag}/\text{AgCl}}$, (b) anodic range $-250 \text{ mV}_{\text{Ag}/\text{AgCl}}$.

Summary

Cavitation studies with MAB in seawater by ultrasound have shown that an etching effect appears, revealing the microstructure of the bronze.

It was found that the κ -phase is attacked the most, and the β -phase more than the α -phase. After tests with the sonotrode, the κ -phase appears to be broken out from the matrix. This could be due to preferential local vapor bubble formation at the κ -phase and the destructive effect of the resulting cavitation impacts.

Potentiostatic experiments indicate the US-enhanced mass transport of oxygen to, and metal ions from the surface being responsible for the US-assisted etching of MAB in seawater under open circuit conditions, the enhanced oxygen supply dominates, resulting in a more anodic free corrosion potential.

References

- [1] X. Y. Li, Y. G. Yan, L. Ma, Z. M. Xu, J. G. Li, Cavitation erosion and corrosion behavior of copper-manganese-aluminum alloy weldment, *Mater. Sci. Eng. A* 382, (2004) 1/2, 82-89.
- [2] Z. Qin, Q. Zhang, Q. Luo, Z. Wu, B. Shen, L. Liu, W. Hu, Microstructure design to improve the corrosion and cavitation corrosion resistance of a nickel-aluminum bronze, *Corrosion Science* 139 (2018) 255-266.
- [3] P. Brezina, Heat treatment of complex aluminium bronzes, *Int. Met. Rev.* 27 (1982) 77-120.
- [4] E. A. Culpan, G. Rose, Corrosion Behaviour of Cast Nickel Aluminium Bronze in Sea Water, *J. Mater. Sci.* 13 (1978) 8, 1647-1657.
- [5] F. Hasan, A. Jahanafrooz, G. W. Lorimer, N. Ridley, The Morphology, Crystallography, and Chemistry of Phases in As-Cast Nickel-Aluminum Bronze. *Metall. Trans. A.* 13A (1982) 8, 1337-1345.
- [6] I. Cobo, M. V. Biezma Moraleda, L. Sánchez, Estudio microestructural de bronzes de aluminio y níquel (NAB) y bronzes de aluminio y manganeso (MAB): efecto de dos reactivos químicos. *Material-ES 1* (2017) 3, 59-62.
- [7] Q. N. Song, N. Xu, X. Jiang, Y. Liu, Y. Tong, J. S. Li, Y. F. Bao, Y. X. Qiao, Effect of Sulfide Concentration on the Corrosion and Cavitation Erosion Behavior of a Manganese-Aluminum Bronze in 3.5% NaCl Solution, *J. Mater. Eng. Perform.* 28 (2019) 4053-4064.
- [8] P. Linhardt, S. Strobl, J. Böhm, M. V. Biezma Moraleda, R. Haubner, Heat Treatment Effect on the Microstructure and the Corrosion Resistance of Manganese-Aluminum Bronzes *Practical Metallography*, 58 (2021) 72-82.
- [9] N. M. Mota, S. S. M. Tavares, A. Nascimento, G. Zeeman, M. V. Biezma Moraleda, Failure analysis of a butterfly valve made with Nickel Aluminum Bronze (NAB) and Manganese Aluminum Bronze (MAB), *Engineering Failure Analysis*, 129 (2021) 105732.
- [10] M. V. Biezma Moraleda, P. Linhardt, S. Strobl, R. Haubner, Influence of Annealing Treatments on Welded CuNi Sheets on the Corrosion Behaviour in Sea Water, *BHM Berg- und Hüttenmännische Monatshefte*, 166 (2021) 434-442.
- [11] J. Böhm, P. Linhardt, S. Strobl, R. Haubner, M. V. Biezma Moraleda, Microstructure of a Heat Treated Nickel-Aluminum Bronze and Its Corrosion Behavior in Simulated Fresh and Sea Water. *Materials Performance and Characterization*, 5 (2016) 689-700.
- [12] I. Cobo Ocejó, M. V. Biezma Moraleda, P. Linhardt, Corrosion Behavior of Heat-Treated Nickel-Aluminum Bronze and Manganese-Aluminum Bronze in Natural Waters, *Metals* (2022) 12, 380.
- [13] K. R. Trethewey, T. J. Haley, C. C. Clark, Effect of ultrasonically induced cavitation on corrosion behaviour of a copper-manganese-aluminium alloy. *Br. Corros. J.* 23 (1988) 1, 55-60.
- [14] M. V. Biezma, O. Gómez de la Rasilla, R. Haubner, P. Linhardt, Etching of Manganese Aluminum Bronze by Ultrasound in Seawater, *Practical Metallography*, 59 (2022) 236-250.
- [15] G. F. Vander Voort, *Metallography—Principles and Practice*, 3rd ed., ASM International, Materials Park, OH, 2004.